Atomic layer deposition of Al_2O_3 and TiO_2 on MoS_2 surfaces

Jaron A. Kropp, Yuhang Cai, Zihan Yao, Wenjuan Zhu, and Theodosia Gougousi

Citation: Journal of Vacuum Science & Technology A **36**, 06A101 (2018); doi: 10.1116/1.5043621
View online: https://doi.org/10.1116/1.5043621
View Table of Contents: http://avs.scitation.org/toc/jva/36/6
Published by the American Vacuum Society

Articles you may be interested in

Rapid atomic layer etching of Al_2O_3 using sequential exposures of hydrogen fluoride and trimethylaluminum with no purging
Journal of Vacuum Science & Technology A **36**, 061508 (2018); 10.1116/1.5043488

Ab initio analysis of nucleation reactions during tungsten atomic layer deposition on Si(100) and W(110) substrates
Journal of Vacuum Science & Technology A **36**, 061507 (2018); 10.1116/1.5044740

Plasma-enhanced atomic layer deposition of titanium vanadium nitride
Journal of Vacuum Science & Technology A **36**, 06A103 (2018); 10.1116/1.5037463

Thermal atomic layer etching of HfO_2 using HF for fluorination and $TiCl_4$ for ligand-exchange
Journal of Vacuum Science & Technology A **36**, 061504 (2018); 10.1116/1.5045130

In situ XPS study of low temperature atomic layer deposition of B_2O_3 films on Si using BCl_3 and H_2O precursors
Journal of Vacuum Science & Technology A **36**, 061503 (2018); 10.1116/1.5044396

Review Article: Atomic layer deposition for oxide semiconductor thin film transistors: Advances in research and development
Journal of Vacuum Science & Technology A **36**, 060801 (2018); 10.1116/1.5047237

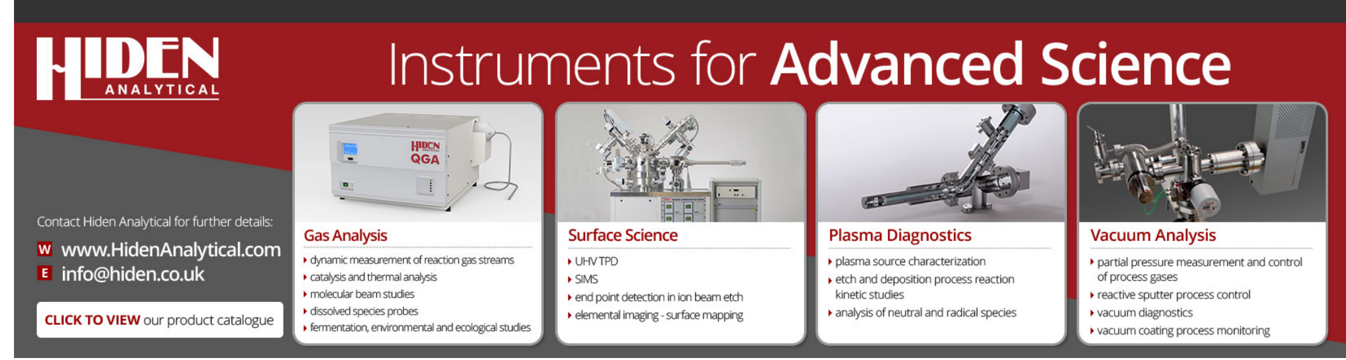

Atomic layer deposition of Al_2O_3 and TiO_2 on MoS_2 surfaces

Jaron A. Kropp,[1] Yuhang Cai,[2] Zihan Yao,[2] Wenjuan Zhu,[2] and Theodosia Gougousi[1,a)]
[1]*Department of Physics, UMBC, Baltimore, Maryland 21250*
[2]*Department of Electrical and Computer Engineering, University of Illinois at Urbana-Champaign, Urbana, Illinois 61801*

(Received 11 June 2018; accepted 7 September 2018; published 4 October 2018)

In this work, the authors compare the surface coverage obtained in the initial and intermediate steps of Al_2O_3 and TiO_2 atomic layer deposition on MoS_2 surfaces prepared by either mechanical exfoliation or chemical vapor deposition (CVD). They find that the film surface coverage is highly dependent on the origin and preparation of the MoS_2 starting surface. While mechanical exfoliation can be used to quickly obtain few-layer MoS_2 surfaces, these surfaces exhibit significant variability in quality and cleanliness, leading to unpredictable film growth. Conversely, MoS_2 grown by CVD provides a more reliable starting surface resulting in significantly improved scattering in the surface coverage. They find that, on CVD MoS_2, neither Al_2O_3 nor TiO_2 film growth strongly exhibits temperature dependence described by the Langmuir adsorption model. For both processes, films up to 6 nm thick deposited on CVD MoS_2 are not fully coalesced and exhibit a large concentration of pinhole type features. *Published by the AVS.* https://doi.org/10.1116/1.5043621

I. INTRODUCTION

Two-dimensional semiconductors such as MoS_2 have attracted considerable interest in recent years due to their novel electronic properties. Comparable in structure to graphene[1] but with an indirect bandgap of ~1.29 eV in bulk form and a direct bandgap of ~1.9 eV in monolayer form,[2] MoS_2 is a natural candidate for a channel material in thin-film field effect transistors (FETs). In fact, the fabrication and performance of devices derived from MoS_2, including but not limited to FETs, have been the subject of much study of late.[3–16] One of the most important elements of many of these devices is a high-quality dielectric film on top of the semiconducting MoS_2 layer. Atomic layer deposition (ALD) is often used to deposit high-k dielectric films on MoS_2 for this purpose.[4,7,8,11,13–23] However, the lack of dangling bonds on the MoS_2 surface results in poor reaction between the surface and the ALD precursors. This typically leads to incomplete surface coverage for dielectric films up to ~15 nm thick unless the surface is treated in some way before deposition.[4,8,14,15,17–25] This presents a substantial problem for nanoelectronic devices, i.e., FETs where dielectric gate thicknesses below 10 nm are desired. To enable reliable production of MoS_2-based devices, a complete understanding of the ALD process chemistry on the MoS_2 surface is required. However, due to the large variety of surface preparation techniques, it can be difficult to discern the exact reaction mechanisms.

Few-layer or monolayer MoS_2 may be prepared by mechanical exfoliation (the "Scotch tape" method) which itself has several variations[26–28] or synthesized by chemical vapor deposition (CVD).[29–33] Both preparation methods create surfaces with a variety of defects.[34–37] The presence of both defects and contamination from either the exfoliation process or the vapor deposition process can affect greatly the quality and reactivity of the starting MoS_2 surface. In ALD, the film nucleation step relies on the presence of suitable functional groups on the starting surface. As a result, the presence of contaminants on the surface that may either promote or inhibit film nucleation and growth may lead to erroneous conclusions about the effectiveness of any surface preparation approaches employed. In this paper, we investigate the high degree of variation found in both exfoliated and CVD-grown MoS_2 surfaces through characterization of ALD-grown dielectric films. We also compare ALD processes using alkyl and alkyl amine precursors.

II. EXPERIMENT

Molybdenum disulfide multilayers were exfoliated from a bulk crystal (SPI Supplies) using Scotch tape or semiconductor dicing tape (Semiconductor Equipment Corp.) and transferred to 300 nm SiO_2/Si substrates. Samples were annealed for 30 s on a 100 °C hotplate prior to removal of the tape to improve the adhesion of MoS_2 to the substrate. This method was modified from the technique outlined by Huang *et al.*[27]

Monolayer MoS_2 was grown on 280–300 nm SiO_2/Si substrates using a CVD method. Molybdenum trioxide (MoO_3) powder (0.060 g) and sulfur (S) powder (0.400 g) were used as the precursors. The substrates were placed face down above the MoO_3 powder at the center of a tube furnace and heated to ~730 °C while the S powder was placed upstream and heated to 200 °C. The growth duration was ~5 min. Argon carrier gas was flowed at 490 sccm during the entire process. MoS_2 samples were imaged optically using a Nikon Digital Sight camera connected to a Nikon Optiphot-100 microscope. The Raman spectra were measured using an Horiba Raman Confocal Imaging Microscope.

Al_2O_3 and TiO_2 films were deposited on multilayer (exfoliated) and monolayer (CVD-grown) MoS_2 samples using trimethyl aluminum (TMA) and tetrakis dimethylamino titanium (TDMAT), respectively, as precursors with water as the oxidizer. Films were grown at 100–200 °C in a custom-built ALD reactor described previously by Henegar and

[a)]Electronic mail: gougousi@umbc.edu

Gougousi.[38] Samples were heated for 30 min in the reactor to reach thermal equilibrium before the depositions began. The precursor (TMA or TDMAT) and water were introduced under 17 sccm nitrogen flow by short pulses, separated by a 30 s nitrogen purge. Film thickness and growth rates were measured using spectroscopic ellipsometry (JA Woollam α-SE) on companion native oxide Si(100) wafer pieces.

After the film deposition, MoS_2 samples were characterized via atomic force microscopy (AFM) using a Veeco Dimension 3100 AFM. AFM images were processed using the WSXM software package.[39] Film surface coverage was calculated from the AFM images using the IMAGEJ software package[40] by first converting the images to 8-bit grayscale and then to binary images using the built-in Sauvola local thresholding algorithm that defines the threshold $T(x,y)$ as

$$T(x, y) = m(x, y) \times \left[1 + k\left(\frac{s(x, y)}{R} - 1\right)\right], \quad (1)$$

where $m(x,y)$ is the local mean and $s(x,y)$ is the local standard deviation of the image.[41] The parameter R is the dynamic range of the standard deviation and was left at the default value of $R = 128$. Images with low surface coverage were used to set the value for parameter k. A value of $k = 0.3$ was found to produce the best match between the primary and binary images. Surface coverage was measured from the binary images. These values ($R = 128$ and $k = 0.3$) were used for all image quantification. Varying the k parameter by ±33% (from 0.2 to 0.4) results in changes of no greater than ±5% in measured surface coverage.

III. RESULTS

A. Surface preparation

CVD-grown MoS_2 flakes were characterized using optical microscopy [Fig. 1(a)], Raman spectroscopy [Fig. 1(b)], and AFM [Figs. 1(c) and 1(d)]. The optical image in Fig. 1(a) shows the edge of a continuous MoS_2 region (left) and the presence of several isolated, triangular flakes with linear dimensions of ~50 μm. Typical flake sizes range from 10 to 50 μm. The spacing between the A_{1g} and E_{2g} Raman modes shown in Fig. 1(c) is ~18 cm^{-1} which is indicative of monolayer MoS_2.[42,43] Using AFM, the flake height [Fig. 1(c)] is measured to be ~0.7 nm which is very near to the expected thickness for a monolayer of MoS_2.[34,44] The root mean square (RMS) roughness of the flake in Fig. 1(d) is measured as 0.165 nm.

Mechanical exfoliation using adhesive tape is a relatively straightforward way to achieve large area (~25 μm^2) few-layer MoS_2 flakes.[27,28] The method entails removing layers of material from a bulk MoS_2 crystal with a piece of tape. Before transferring to a substrate, the tape-mounted MoS_2 may be thinned ~5–20 times with a clean piece of tape. The tape-mounted MoS_2 is then pressed to the substrate (usually SiO_2/Si) and rubbed with tweezers or another object to encourage van der Waals interactions between the MoS_2 and the SiO_2. The tape is carefully removed, leaving behind MoS_2 layers of varying size and thickness. While this

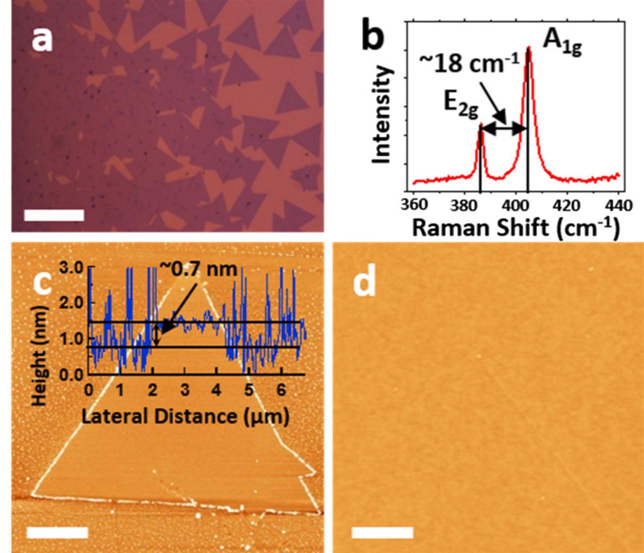

FIG. 1. Characterization of CVD-grown MoS_2. (a) Optical micrograph of MoS_2 flakes on 300 nm SiO_2 substrate (scale bar 50 μm) and (b) Raman spectrum of the E_{2g} and A_{1g} modes of MoS_2. AFM images of a typical flake and its surface is shown in (c) (scale bar 2 μm) and (d) (scale bar 600 nm), respectively. The flake height was measured as ~0.7 nm in (c), and the RMS roughness from (d) was measured as 0.165 nm.

method has been shown to produce large area, thin MoS_2 flakes, the tape can leave behind significant adhesive residue. Additionally, the exfoliated MoS_2 surfaces have been shown to contain a large number of defects, which are primarily sulfur vacancies.[34,37] Typically, adhesive residues are cleaned by soaking the samples in acetone for up to 8 h.[18,20,22,25] However, we found that long soaks in acetone can cause increased contamination of the MoS_2 surface. In Fig. 2, an exfoliated sample has been imaged just after exfoliation with Scotch tape and again after several hours of soaking in acetone (Fisher Scientific, ACS grade). Each acetone soak was followed by a 1 min rinse in acetone, methanol (Fisher Scientific, lab grade), and deionized water (Neu Ion).

The adhesive leaves behind residue that appears bright yellow-green on the MoS_2 flake (blue-green) and on the Si substrate. After 4 h in acetone, the amount of visible adhesive residue on the flake has decreased, but after a total of 8 h, the contamination covers more of the MoS_2 surface than it initially had. AFM [Fig. 2(d)] reveals that in addition to the bands of adhesive visible with optical imaging, there is the possibility of further surface contamination by adhesive fragmentation/decomposition byproducts that may go undetected in the optical image. This series of data shows that the outcome of the acetone cleaning procedure is random; it may produce high-quality surfaces, but it may also result in widespread contamination. As such, unless each flake is examined after the cleaning and prior to the deposition by AFM, there is no certainty for the condition of the starting surface.

B. Atomic layer deposition of Al_2O_3

To investigate the variability in exfoliated MoS_2 surfaces obtained by different preparation methods, we performed 12

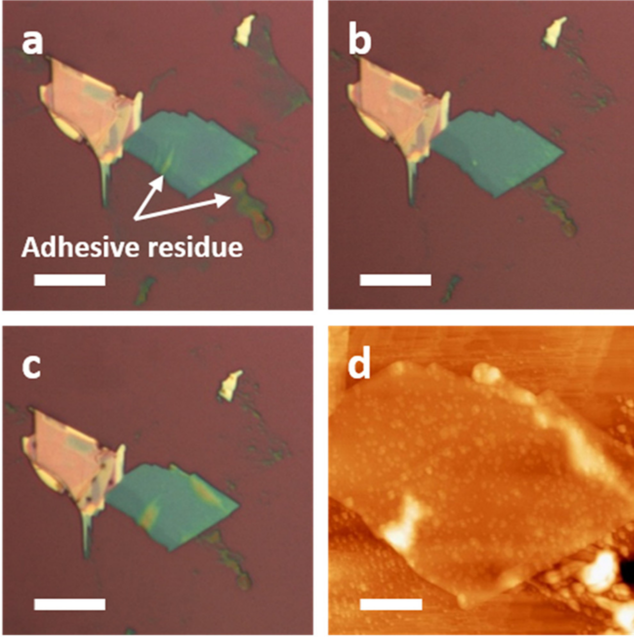

FIG. 2. Optical micrographs of MoS_2 exfoliated with scotch tape and annealed for 120 s on a 100 °C hotplate [(a)–(c)]. The as-exfoliated flake is shown in (a) and the images taken after acetone soaks of 4 and 8 h are shown in (b) and (c), respectively. In (d), an AFM image of the flake after an 8 h acetone soak is shown. Scale bars are 10 μm in [(a)–(c)] and 3 μm in (d).

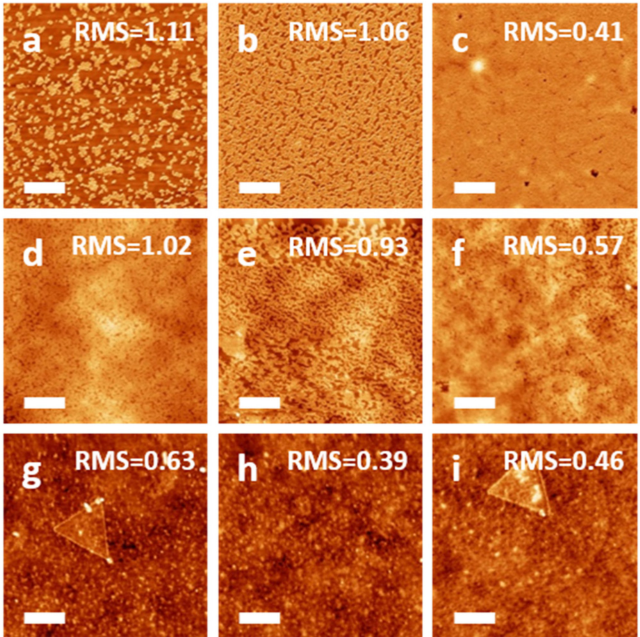

FIG. 3. AFM images of 1 nm Al_2O_3 deposited at 100 °C on dicing tape exfoliated MoS_2 [(a)–(c)], Scotch tape exfoliated MoS_2 [(d)–(f)], and CVD-grown MoS_2 [(g)–(i)]. The scale bar is 600 nm for all images. For each surface preparation, images are taken from different flakes on the same substrate. RMS roughness values are given in units of nm.

ALD cycles of Al_2O_3 at 100 °C on dicing tape exfoliated and Scotch tape exfoliated MoS_2. The growth per cycle (GPC) for this process was measured to be 0.87 Å/cycle on Si/SiO_2 substrates and the expected film thickness was 1 nm. To study the effects of residual contamination caused by the exfoliation, the samples were not cleaned with acetone prior to ALD. To provide a control group, the same deposition was carried out on CVD-grown MoS_2, which is expected to provide more uniform starting surfaces. This low temperature was chosen to ensure that some surface coverage will be obtained. Films of this thickness were not expected to fully cover the surface and should provide insight into the effects of surface preparation on the nucleation mechanisms. The sample morphology after the depositions was investigated by AFM, and a small selection of the data obtained is shown in Fig. 3. AFM scans for each surface preparation were taken from different flakes on the same substrate.

Semiconductor dicing tape was used as an alternative to the standard Scotch tape since the lower tack of the adhesive is expected to provide cleaner transfers. For the samples prepared using the dicing tape [Figs. 3(a)–3(c)], a large variation in Al_2O_3 surface coverage is detected ranging from very low coverage [Fig. 3(a)] to almost complete coverage [Fig. 3(c)]. The data shown in this figure were selected to illustrate the large variation in the deposition outcome. For the samples prepared using Scotch tape [Figs. 3(d)–3(f)], higher coverage was achieved but the films are still not continuous. Many pinholes are visible in these films. For the depositions performed on the CVD flakes, the AFM data show that the film is just beginning to nucleate, with no coalescence of the islands formed. By contrast, the Al_2O_3 film deposited on the 300 nm SiO_2/Si substrate is completely coalesced and relatively smooth [Fig. S1(a)[49]] with an RMS roughness of 0.32 nm.

A quantitative estimate of the surface coverage for these samples is shown in Fig. 4. The results for each exfoliation approach were taken from several flakes on the same SiO_2 substrate to ensure that each flake underwent identical preparation and processing. The control group of CVD MoS_2 flakes shows some scattering (16%–37%) but the surface coverage is low as expected for a 1 nm film. The surfaces

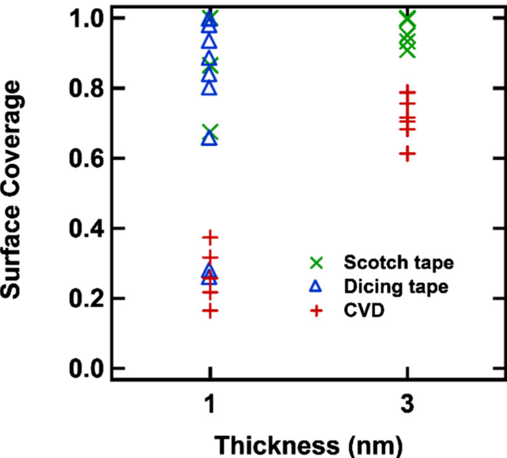

FIG. 4. Calculated surface coverage for 1 and 3 nm Al_2O_3 films grown at 100 °C on Scotch tape exfoliated, dicing tape exfoliated, and CVD-grown MoS_2 surfaces. Error bars are not included for clarity but the uncertainty for the surface coverage is estimated at ~5%.

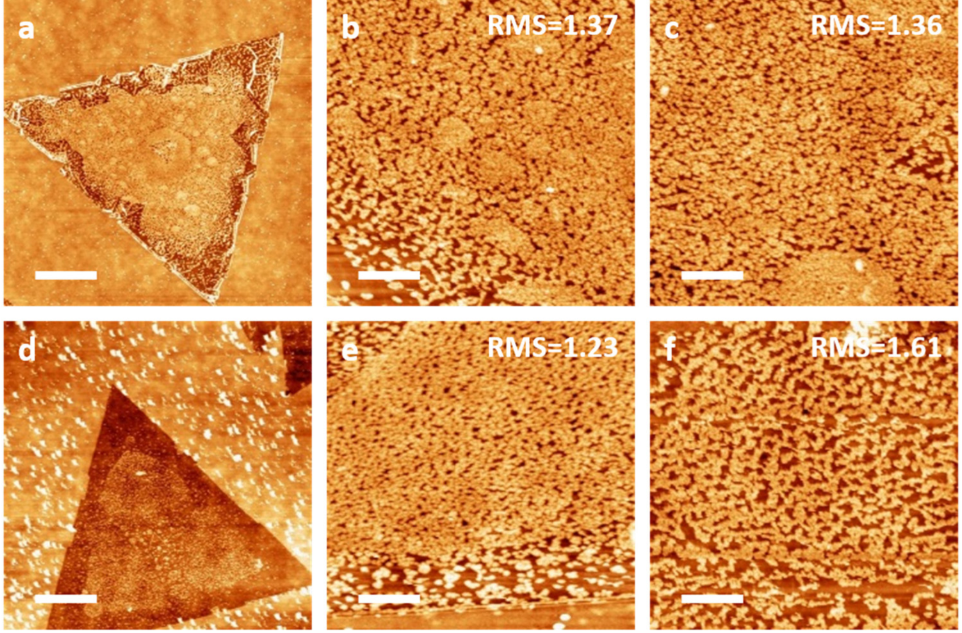

FIG. 5. AFM images of 3 nm Al_2O_3 deposited on CVD-grown MoS_2 at 100 °C [(a)–(c)] and 200 °C [(d)–(f)]. Scale bars are 3 μm [(a), (d)] and 600 nm [(b), (c), (e), (f)]. RMS roughness values are given in units of nm.

prepared using dicing tape yield samples with very large scattering in the surface coverage (25%–98%) with more than half of the data points clustering above 80%. The data set obtained from the Scotch tape samples is smaller but also tends to cluster at the high (>70%) surface coverage region.

Subsequently the morphology of thicker films (35 cycles, ~3 nm) was examined, as such films are expected to be continuous and provide uniform surface coverage when grown on hydrophilic surfaces such as SiO_2 [Fig. S1(b)[49]]. AFM images of 3 nm Al_2O_3 films deposited on CVD MoS_2 at 100 °C are shown in Figs. 5(a)–5(c), and while regions of dense film coalescence can be found in any single flake, the films are in general not continuous, with surface coverage ranging from 61% to 79% (Fig. 4). We find that denser coverage is obtained at the center of the triangular flake and the coverage drops substantially closer to the flake edges. The CVD flakes were prepared on SiO_2, and Fig. 5(a) shows the contrast in the behavior of the MoS_2 and the SiO_2 surface. The area surrounding the MoS_2 flake is covered with a fairly smooth layer of Al_2O_3. For a set of samples prepared on exfoliated flakes, higher surface coverage (90%–99%; Fig. 4) was measured, as expected from the results with the 1 nm films.

To investigate the effect of temperature on the film nucleation, another set of 3 nm Al_2O_3 films (30 cycles, GPC 1.0 Å/cycle) was deposited on CVD MoS_2 flakes at 200 °C and AFM data for a few of the samples are included in Figs. 5(d)–5(f). AFM scans at each temperature were taken from different flakes on the same substrate. Comparing the data at the two temperatures, some variation in the surface coverage is observed. For both process temperatures, the Al_2O_3 film preferentially grows in the center of the flake, avoiding the edge regions. The film coverage at 100 °C ranges from 61% to 79%, while at 200 °C, the coverage ranges from 54% to 75% [Fig. S2 (Ref. 49)].

While CVD-grown MoS_2 flakes offer a more controlled environment to study the nucleation of dielectrics during the ALD process, they are not completely free of defects.[31,35,37] Figure 6 includes some sample AFM data taken after the deposition of 3 nm of Al_2O_3 at 100 °C. The film grows along grain boundaries [Figs. 6(a) and 6(b)] and along the edges of a multilayered triangular region often found in the center of CVD-grown MoS_2 flakes [Fig. 6(b)].

C. Atomic layer deposition of TiO_2

TMA is a very aggressive alkyl precursor that reacts with a variety of surfaces even at temperatures below 100 °C. Alkyl amine precursors are also used for a variety of ALD dielectric processes, so we chose to compare the reactivity and surface chemistry of the two precursor classes using the CVD-grown MoS_2 monolayer surfaces. For that purpose, we deposited TiO_2 films on CVD MoS_2 at 100–200 °C using TDMAT and water. The ideal temperature for the TDMAT/

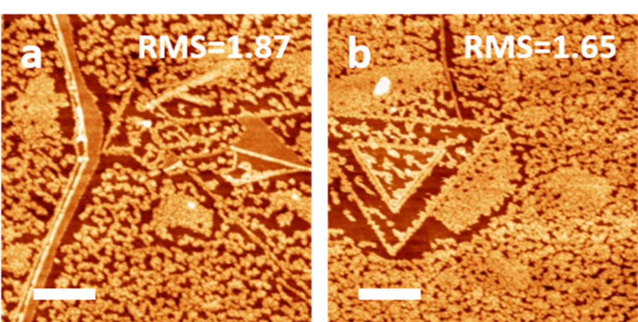

FIG. 6. AFM images of 3 nm Al_2O_3 films grown on CVD MoS_2 at 100 °C showing growth along defects (a) and multilayered step edges (b). Scale bars are 600 nm. RMS roughness values are given in units of nm.

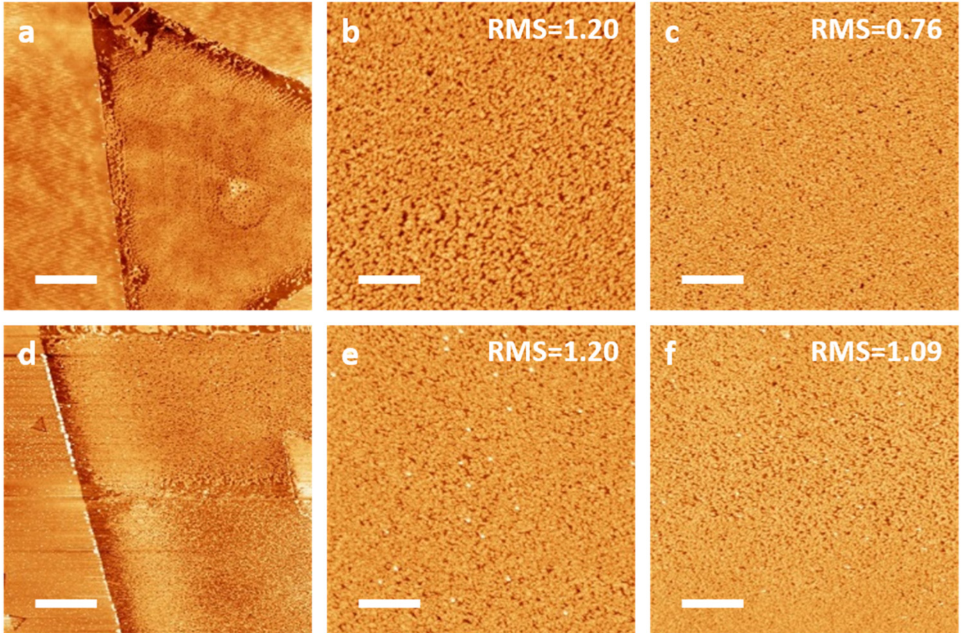

FIG. 7. AFM images of 3 nm TiO_2 deposited on CVD-grown MoS_2 at 100 °C [(a)–(c)] and 200 °C [(d)–(f)]. Scale bars are 2 μm [(a), (d)] and 600 nm [(b), (c), (e), (f)]. RMS roughness values are given in units of nm.

H_2O ALD process in our reactor is 200 °C with a nominal growth rate of 0.4 Å/cycle.[45] At 100 °C, the growth rate is 0.6 Å/cycle. The films were grown at thicknesses of 3 nm (50 or 75 cycles at 100 or 200 °C, respectively) and 6 nm (100 or 150 cycles at 100 or 200 °C, respectively). The surface coverage was calculated as before. Some sample AFM images of 3 and 6 nm TiO_2 films grown at both temperatures are shown in Figs. 7 and 8, respectively. AFM scans at a given temperature and thickness were taken from different flakes on the same substrate. Similar to the Al_2O_3 films, the TiO_2 films grow primarily in the center region, avoiding the flake edges. The films deposited at 100 °C appear to have a connected network of voids while the films deposited at 200 °C show more granular structure, with the RMS roughness decreasing marginally as the deposition temperature increases. However, even at 6 nm, the film is not continuous and many pinholes are visible at both deposition temperatures. The surface coverage calculations (Fig. 9)

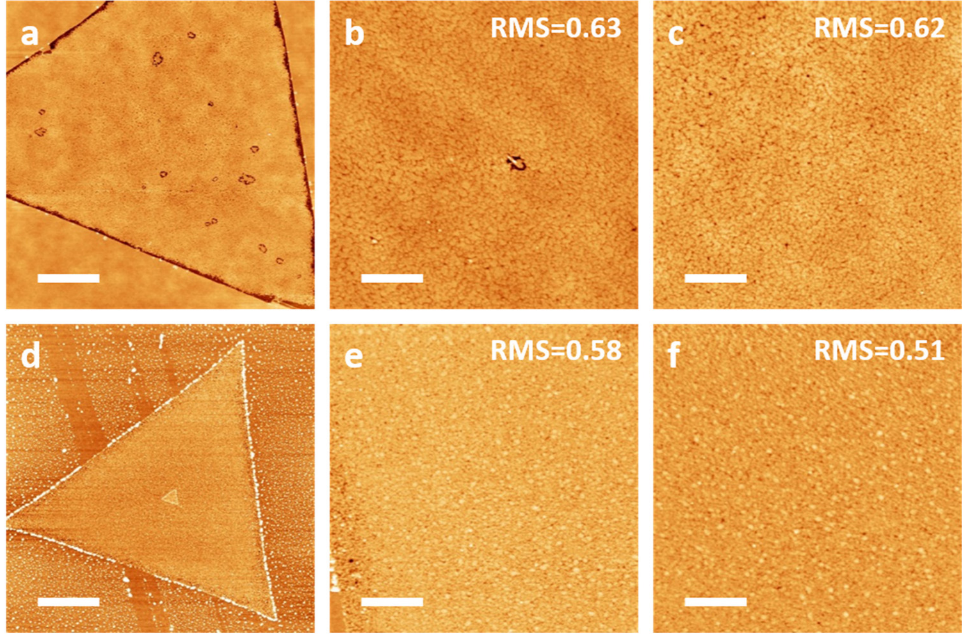

FIG. 8. AFM images of 6 nm TiO_2 deposited on CVD-grown MoS_2 at 100 °C [(a)–(c)] and 200 °C [(d)–(f)]. Scale bars are 2 μm [(a), (d)] and 600 nm [(b), (c), (e), (f)]. RMS roughness values are given in units of nm.

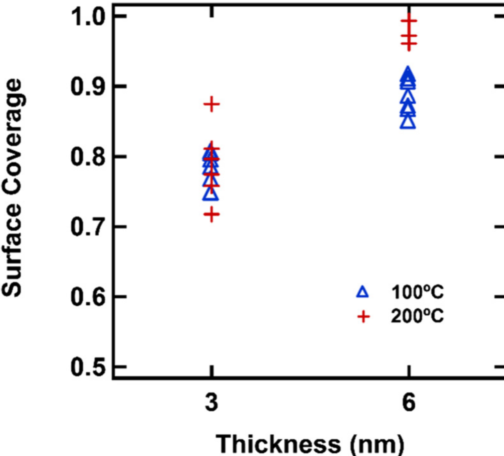

FIG. 9. Calculated surface coverage of 3 and 6 nm TiO_2 deposited on CVD-grown MoS_2 at 100 and 200 °C. Error bars are not included for clarity but the uncertainty for the surface coverage is estimated at ~5%.

show both an overall increase in coverage with film thickness and for 6 nm films, a slight overall increase in coverage with temperature.

IV. DISCUSSION

A. Starting surface variability

Exfoliated MoS_2 flakes with and without further cleaning to remove residual adhesive have been used extensively in the literature. One of the most common cleaning approaches is an hours-long soak of the surfaces in acetone. When similar cleaning approaches were tested in this work, we found that long acetone soaks may redistribute the adhesive residue, resulting in surfaces covered with nanoscale debris [Fig. 2(d)] that may not be visible optically. To study the effect of variations in residual contamination on the surface coverage from exfoliation alone, exfoliated samples were prepared and tested without any cleaning steps. For the deposition of 1 nm nominal thickness of Al_2O_3 on these surfaces, measured coverage ranged from as little as ~25% to nearly complete surface coverage. As the samples were used without attempts to remove the residual adhesive from the exfoliation, this result can be attributed to the significant differences in the level of contamination from sample to sample. Previously, ~10 nm Al_2O_3 films were shown to grow uniformly on MoS_2.[18] It has been suggested that this may be a result of the solvent-based cleaning steps performed after mechanical exfoliation.[19,24] That, along with the data presented here, suggests that increased surface contamination may also contribute to the continuous growth of ALD films by serving as nucleation sites. Additionally, we observe some differences in the amount of scattering in the measured surface coverage between samples prepared by exfoliation using semiconductor dicing tape and those prepared using Scotch tape. The Scotch tape exfoliated samples exhibit greater surface coverage of 1 nm Al_2O_3 overall, suggesting that the average level of contamination is higher than that on dicing tape prepared samples where very low film coverage (25%) has been observed. The scattering in the surface coverage on the dicing tape exfoliated surfaces is large (25%–98%) indicating that, while relatively clean surfaces may be obtained through this method, its reliability is poor.

In addition to the possible presence of residual adhesive, mechanically exfoliated MoS_2 exhibits surface defects (mainly sulfur vacancies) at concentrations between 0.1% and 10%.[34,37] Density functional theory calculations have shown that dissociation of molecular oxygen can occur at sulfur vacancies, allowing atomic oxygen to adsorb on the vacancy site.[46] TMA is a known oxygen scavenger and we expect that the oxygen-filled vacancies may react more readily with TMA and seed the film growth. The combination of the presence of surface contamination and a large concentration of sulfur vacancies may explain the very high surface coverage obtained for the deposition of 1 nm of Al_2O_3 on the exfoliated samples (Fig. 4). By comparison, when 1 nm of Al_2O_3 was deposited at 100 °C on CVD-grown MoS_2, the surface coverage was significantly lower with less scattering. While these CVD-grown samples are not free of defects, the initial surface condition is more reproducible and these surfaces present the opportunity to study the ALD process surface chemistry in a more controlled setting.

B. Al_2O_3 and TiO_2 films on CVD-grown MoS_2

ALD of Al_2O_3 films on MoS_2 has been shown previously to be dominated by precursor physisorption and, therefore, surface coverage is expected to decrease with deposition temperature.[18,20,24] This temperature dependence was previously explained by Park *et al.* using the Langmuir adsorption model,[20] where the desorption of precursor molecules from the surface depends on the substrate temperature (T) and the desorption energy (E_{des}). Park *et al.* state that the uncovered fraction of the surface is proportional to $\exp(-E_{des}/k_BT)$. Assuming no chemisorption, the adsorption energy of precursor molecules (E_{ads}) is approximately equal to E_{des}, so the initial surface coverage in the limit of pure physisorption depends only on E_{ads} of the precursor and the substrate temperature. In this work, 3 nm Al_2O_3 films deposited on CVD-grown MoS_2 at 100 °C have surface coverage from 61% to 79% with an average coverage of 71% (Fig. 4) while analogous films deposited at 200 °C have surface coverage from 54% to 75% [average 66%; Fig. S2 (Ref. 49)]. Elevated deposition temperature leads to marginally reduced surface coverage as expected by the simple Langmuir model. However, the scattering in the data is such that no conclusion about the degree of contribution of this mechanism can be made. CVD-grown MoS_2 surfaces are free from organic adhesive but they may have some residual surface variation from the presence of the species used in the growth. These surfaces also contain defect sites as well as grain boundaries.[31,35,37] The scatter in the data is presumed to originate from such nonideal starting surfaces as shown in Fig. 6. These factors are not accounted for in the simple Langmuir adsorption model described above. The high variability in

surface coverage indicates that temperature-dependent physisorption is not as important as the quality of the starting surface. Since common defects such as sulfur vacancies are easily passivated with oxygen,[46] these sites react readily with the ALD precursors and seed the film growth.

To study the effects of precursor choice on film growth, we deposited TiO_2 films on CVD MoS_2 using TDMAT and water. TDMAT is an alkyl amine precursor, and thus, this process is representative of ALD processes using similar alkyl amine precursors. Several dielectric materials of interest in nanoelectronics can be grown with such precursors, including HfO_2 and ZrO_2.[47] TiO_2 films were grown at a nominal thickness of 3 nm at both 100 and 200 °C. Film growth was expected to be dominated by precursor physisorption, and thus, the surface coverage should decrease as temperature increases. However, at both temperatures, the average TiO_2 surface coverage is ∼78%. The lack of any clear temperature dependence suggests that there are competing mechanisms during the growth of TiO_2 on MoS_2. The average surface coverage of TiO_2 films is slightly higher than that of Al_2O_3 by ∼8%–12%, though the range of coverage does overlap. It is therefore difficult to discern any precursor-dependent effects from surface coverage measurements alone. It is possible that there are some differences in the initial reaction of TMA/TDMAT with the MoS_2 surface. The AFM images in Figs. 5(e) and 5(f), for example, show Al_2O_3 films with large gaps, while the TiO_2 films in Figs. 7(e) and 7(f) are visibly different, with smaller gaps between coalesced islands.

Deeper insight into the growth mechanics of TiO_2 on MoS_2 can be gained from the deposition of the thicker 6 nm TiO_2 films grown at 100 and 200 °C. The surface coverage for these films increases as a function of temperature (Fig. 9), defying the Langmuir adsorption model. The increased surface coverage at elevated temperature suggests that at 200 °C the reaction between TDMAT and MoS_2 is thermally activated. Diffusion is also thermally activated, and an increase in the surface temperature may result in enhanced diffusion of the TDMAT molecules on the surface before finding a favorable bonding site (i.e., a defect or –OH terminated site). Since bonding to edge sites is energetically favorable compared to bonding to terrace sites, enhanced diffusion should result in smoother films and increased surface coverage which is observed for the films deposited at 200 °C [Figs. 8(e) and 8(f)]. Additionally, Fig. 8(d) shows that the TiO_2 film has grown nearly to the edge of the MoS_2 flake, in contrast to the flake in Fig. 8(a), where the film has not migrated to the flake edge. The fact that TiO_2 film coverage increases with temperature further suggests differences between the reactions of TMA and TDMAT with MoS_2. However, elucidation of the exact differences in TMA/TDMAT reactions with the MoS_2 surface requires further study.

Though the TDMAT/H_2O process yields slightly better film coverage than the TMA/H_2O process on monolayer MoS_2, the TiO_2 films are not completely uniform or pinhole-free even at a thickness of 6 nm. It is, of course, well known that ALD films of Al_2O_3 or HfO_2 on MoS_2 below ∼15 nm in thickness rarely achieve complete, uniform surface coverage without some kind of surface treatment or special deposition conditions.[8,14,15,17–25] This is in contrast to ALD of metal oxides on other hydrophobic surfaces, namely, H-terminated silicon. ALD of HfO_2 on H-terminated Si using tetrakis dimethylamino hafnium and H_2O was found to have a growth barrier for approximately the first four ALD cycles.[48] After 25 cycles, however, the HfO_2 film is continuous with a ∼10 Å interfacial SiO_2 layer between the Si substrate and the HfO_2 film. The formation of this SiO_2 interfacial layer provides the necessary OH surface groups to allow for proper HfO_2 film nucleation. The lack of ability of the MoS_2 basal plane to oxidize readily (except at defect sites) means that no interfacial layer is formed during ALD and substrate-inhibited growth occurs up to 100 ALD cycles or more.

V. CONCLUSIONS

We have studied the ALD of Al_2O_3 on mechanically exfoliated and CVD-grown MoS_2 and the ALD of TiO_2 on CVD-grown MoS_2. There is a high degree of variability in the surface coverage of Al_2O_3 films on exfoliated MoS_2 surfaces due to variations in the starting surfaces, likely caused by residual contamination and defects. CVD-grown MoS_2 shows less variation and thus more reproducible surfaces for the study of the ALD process chemistry. We find that neither Al_2O_3 nor TiO_2 films strongly follow the temperature dependence described by Langmuir adsorption; however, morphological differences between Al_2O_3 and TiO_2 films point to differences in the underlying surface reaction between TMA/MoS_2 and TDMAT/MoS_2.

ACKNOWLEDGMENTS

J.A.K. and T.G. acknowledge support from the National Science Foundation under Grant No. ECCS-1407677. Y.C., Z.Y., and W.Z. would like to acknowledge support from the National Science Foundation under Grant No. ECCS-1611279 and the Office of Naval Research under Grant No. NAVY N00014-17-1-2973.

[1]K. S. Novoselov, D. Jiang, F. Schedin, T. J. Booth, V. V. Khotkevich, S. V. Morozov, and A. K. Geim, Proc. Natl. Acad. Sci. U. S. A. **102**, 10451 (2005).
[2]K. F. Mak, C. Lee, J. Hone, J. Shan, and T. F. Heinz, Phys. Rev. Lett. **105**, 136805 (2010).
[3]B. Radisavljevic, A. Radenovic, J. Brivio, V. Giacometti, and A. Kis, Nat. Nanotechnol. **6**, 147 (2011).
[4]J.-G. Song *et al.*, ACS Appl. Mater. Interfaces **8**, 28130 (2016).
[5]X.-J. Song, L.-C. Xu, H.-F. Bai, Y. Li, Z. Ma, Z. Yang, R. Liu, and X. Li, J. Appl. Phys. **121**, 144505 (2017).
[6]Q. H. Wang, K. Kalantar-Zadeh, A. Kis, J. N. Coleman, and M. S. Strano, Nat. Nanotechnol. **7**, 699 (2012).
[7]K. M. Price, K. E. Schauble, F. A. McGuire, D. B. Farmer, and A. D. Franklin, ACS Appl. Mater. Interfaces **9**, 23072 (2017).
[8]W. Yang, Q.-Q. Sun, Y. Geng, L. Chen, P. Zhou, S.-J. Ding, and D. W. Zhang, Sci. Rep. **5**, 11921 (2015).
[9]Z. Yang, R. Grassi, M. Freitag, Y.-H. Lee, T. Low, and W. Zhu, Appl. Phys. Lett. **108**, 083104 (2016).
[10]W. Zhu, T. Low, Y.-H. Lee, H. Wang, D. B. Farmer, J. Kong, F. Xia, and P. Avouris, Nat. Commun. **5**, 3087 (2014).

[11]H. Liu and P. D. Ye, IEEE Electron Device Lett. **33**, 546 (2012).
[12]W. Park, J.-W. Min, S. F. Shaikh, and M. M. Hussain, Phys. Stat. Sol. A **214**, 1700534 (2017).
[13]Y. Pak *et al.*, Small **14**, 1703176 (2018).
[14]P. Bolshakov, P. Zhao, A. Azcatl, P. K. Hurley, R. M. Wallace, and C. D. Young, Microelectron. Eng. **178**, 190 (2017).
[15]Q. Qian, B. Li, M. Hua, Z. Zhang, F. Lan, Y. Xu, R. Yan, and K. J. Chen, Sci. Rep. **6**, 27676 (2016).
[16]M. Wen, J. Xu, L. Liu, P. T. Lai, and W. M. Tang, IEEE Trans. Electron Devices **64**, 1020 (2017).
[17]L. Cheng, X. Qin, A. T. Lucero, A. Azcatl, J. Huang, R. M. Wallace, K. Cho, and J. Kim, ACS Appl. Mater. Interfaces **6**, 11834 (2014).
[18]H. Liu, K. Xu, X. Zhang, and P. D. Ye, Appl. Phys. Lett. **100**, 152115 (2012).
[19]S. McDonnell *et al.*, ACS Nano **7**, 10354 (2013).
[20]T. Park *et al.*, RSC Adv. **7**, 884 (2017).
[21]Q. Qian, Z. Zhang, M. Hua, G. Tang, J. Lei, F. Lan, Y. Xu, Ruyue Yan, and K. J. Chen, Nanotechnology **28**, 175202 (2017).
[22]S. Son, S. Yu, M. Choi, D. Kim, and C. Choi, Appl. Phys. Lett. **106**, 021601 (2015).
[23]H. Zhang *et al.*, J. Chem. Phys. **146**, 052810 (2016).
[24]A. Azcatl *et al.*, Appl. Phys. Lett. **104**, 111601 (2014).
[25]J. Yang, S. Kim, W. Choi, S. H. Park, Y. Jung, M.-H. Cho, and H. Kim, ACS Appl. Mater. Interfaces **5**, 4739 (2013).
[26]K. S. Novoselov, A. K. Geim, S. V. Morozov, D. Jiang, Y. Zhang, S. V. Dubonos, I. V. Grigorieva, and A. A. Firsov, Science **306**, 666 (2004).
[27]Y. Huang, E. Sutter, N. N. Shi, J. Zheng, T. Yang, D. Englund, H.-J. Gao, and P. Sutter, ACS Nano **9**, 10612 (2015).
[28]G. Z. Magda, J. Pető, G. Dobrik, C. Hwang, L. P. Biró, and L. Tapasztó, Sci. Rep. **5**, 14714 (2015).
[29]Y.-H. Lee *et al.*, Adv. Mater. **24**, 2320 (2012).
[30]K.-K. Liu *et al.*, Nano Lett. **12**, 1538 (2012).
[31]S. Najmaei *et al.*, Nat. Mater. **12**, 754 (2013).
[32]Y. Zhan, Z. Liu, S. Najmaei, P. M. Ajayan, and J. Lou, Small **8**, 966 (2012).
[33]D. Dumcenco *et al.*, ACS Nano **9**, 4611 (2015).
[34]R. Addou, L. Colombo, and R. M. Wallace, ACS Appl. Mater. Interfaces **7**, 11921 (2015).
[35]W. Zhou *et al.*, Nano Lett. **13**, 2615 (2013).
[36]S. Zhou, S. Wang, H. Li, W. Xu, C. Gong, J. C. Grossman, and J. H. Warner, ACS Omega **2**, 3315 (2017).
[37]J. Hong *et al.*, Nat. Commun. **6**, 6293 (2015).
[38]A. J. Henegar and T. Gougousi, Appl. Surf. Sci. **390**, 870 (2016).
[39]I. Horcas, R. Fernández, J. M. Gómez-Rodríguez, J. Colchero, J. Gómez-Herrero, and A. M. Baro, Rev. Sci. Instrum. **78**, 013705 (2007).
[40]W. S. Rasband, *ImageJ* (U.S. National Institutes of Health, Bethesda, MD, 1997).
[41]J. Sauvola and M. Pietikäinen, Pattern Recognit. **33**, 225 (2000).
[42]C. Lee, H. Yan, L. E. Brus, T. F. Heinz, J. Hone, and S. Ryu, ACS Nano **4**, 2695 (2010).
[43]M. Placidi *et al.*, 2D Mater. **2**, 035006 (2015).
[44]X. Li and H. Zhu, J. Materiomics **1**, 33 (2015).
[45]A. J. Henegar and T. Gougousi, ECS J. Solid State Sci. Technol. **4**, 298 (2015).
[46]S. Kc, R. C. Longo, R. M. Wallace, and K. Cho, J. Appl. Phys. **117**, 135301 (2015).
[47]D. M. Hausmann and R. G. Gordon, J. Cryst. Growth **249**, 251 (2003).
[48]J. C. Hackley, J. D. Demaree, and T. Gougousi, J. Vac. Sci. Technol. A **26**, 1235 (2008).
[49]See supplementary material at https://doi.org/10.1116/1.5043621 for AFM data of Al_2O_3 and TiO_2 films grown on silicon and of Al_2O_3 grown on CVD MoS_2 at 200 °C.